



## Enhancement of jet-to-wall heat transfer using axisymmetric grooved impinging plates

B. Sagot<sup>a,\*</sup>, G. Antonini<sup>b</sup>, F. Buron<sup>a</sup>

<sup>a</sup>Laboratoire Fluide et Énergétique, Ecole Supérieure des Techniques Aéronautiques et Construction Automobile (ESTACA), 34-36 rue Victor Hugo, 92300 Levallois-Perret, France

<sup>b</sup>Département de Génie des Procédés Industriels, Université de Technologie de Compiègne (UTC), BP 20529-60205 Compiègne Cedex, France

### ARTICLE INFO

#### Article history:

Received 15 July 2008

Received in revised form

24 November 2009

Accepted 19 December 2009

Available online 6 February 2010

#### Keywords:

Jet impingement

Heat transfer enhancement

Groove

Nusselt number correlation

Constant wall temperature

### ABSTRACT

An experimental investigation was carried out to examine the effects of axisymmetric lathe-worked grooves on the impinging jet-to-wall heat transfer, under constant wall temperature conditions. This study covers jet Reynolds numbers, based on the orifice diameter  $D$ , from 15 000 to 30 000, for a given jet-to-wall dimensionless distance  $H/D = 2$ . The grooves have either square or triangular cross-section, with depth  $c = 1$  mm, and pitch  $p = 2$  mm. Under these conditions, we obtained significant heat transfer enhancements, up to 81% as compared with the smooth plate reference case, for a value of the dimensionless plate radius  $R/D = 2$ , a jet Reynolds number  $Re_j = 23$  000, and for square cross-section lathe-worked grooves.

© 2010 Elsevier Masson SAS. All rights reserved.

## 1. Introduction

The impinging jet-to-wall configuration is of interest for many industrial applications, due to the high local heat transfer coefficients obtained at the stagnation point [1–4]. A heat transfer correlation valid for impinging gas jets, under flux imposed boundary conditions, is available in Incropera et al. [5]. In a recent work, Sagot et al. [6] proposed a correlation applicable to the determination of the average heat transfer coefficient between a jet and a smooth plate, at an imposed temperature.

Under the impinging jet flow configuration, the boundary layer development along the plate induces a progressive increase in the gas-to-wall heat transfer resistance, associated with a reduction of the local heat transfer coefficient. Thus, the current literature is mainly devoted to jet-to-wall configurations with a smooth impinging plate radius  $R$  lower than five times the diameter  $D$  of the injector nozzle ( $R/D \leq 5$ ).

Several studies have shown marked effect of surface roughness on the heat transfer enhancement in duct flows. In the impinging jet configuration, the work of Gau and Lee [7] reported that the presence of triangular surface corrugations permits a significant increase of the local heat transfer coefficient. However, their study

was limited to the analysis of the Nusselt number at the stagnation point. These results were confirmed by Hsieh et al. [8] in the case of rectangular and ellipsoidal corrugations, which allowed an increase of 20–30% of the local Nusselt number. Gao et al. [9] showed that the presence on the surface of equally spaced 45° triangular tabs makes it possible to increase the average Nusselt number from 10% to 25%. Their study, carried out with a jet Reynolds number of 23 000, concentrates on  $R/D$  values ranging from 0 to 4.

In the present experimental study, we analyzed the intensification of the average heat transfer coefficient, in comparison with the smooth plate reference configuration, for two types of axisymmetric grooves (square or triangular), for various jet Reynolds numbers, and for  $R/D$  values ranging from 2 to 10.

## 2. Experimental program

Fig. 1 presents the experimental setup used in this study, which involves a hot gas jet impinging on an imposed temperature cold wall. A controlled air flow rate is supplied by a compressed air unit, de-oiled, dried, and heated in a coaxial exchanger ensuring a stable jet temperature. We fixed the flow rate to values ranging from 1.2 to 12  $\text{Nm}^3 \text{h}^{-1}$ .

To minimize the pressure drop in the injection device, the gas was delivered through a 200 mm long thermally insulated pipe, with a large inner diameter (17 mm). An orifice plate is fitted at the end of this central pipe to provide an impinging gas jet. The hot jet

\* Corresponding author.

E-mail address: [benoit.sagot@estaca.fr](mailto:benoit.sagot@estaca.fr) (B. Sagot).

**Nomenclature**

$b$	width of the grooves (see Fig. 2), m
$c$	depth of the grooves, m
$C_p$	gas specific heat, $\text{J kg}^{-1} \text{K}^{-1}$
$D$	jet-orifice diameter (see Fig. 1), m
$D_v$	diameter of the cylindrical vessel, m
$e$	orifice plate thickness, m
$f$	intensification factor (–)
$F$	dimensionless outlet temperature in Eq. (6) (–)
$H$	orifice-to-plate distance, m
$\bar{h}(R)$	average heat transfer coefficient, based on $T_j - T_w$ temperature difference, $\text{W m}^{-2} \text{K}^{-1}$
$K$	dimensionless coefficient in Eq. (9) (–)
$\dot{m}_g$	gas mass flow rate, $\text{kg s}^{-1}$
$n$	exponent in Eq. (9) (–)
$Nu_T(r)$	local Nusselt number at a constant wall temperature, based on $T_j - T_w$ (–)
$\bar{Nu}_T$	average Nusselt number at a constant wall temperature, based on $T_j - T_w$ (–)
$\bar{Nu}'_T$	average Nusselt number at a constant wall temperature, based on $(T_j + T_o)/2 - T_w$ (–)
$p$	grooves pitch, m
$R$	impingement plate radius, m

$r$	radial coordinate, m
$Re_j$	jet Reynolds number (–)
$T$	temperature K
$U_j$	average gas velocity at orifice exit, $\text{m s}^{-1}$

**Greek symbols**

$\delta/2$	radial distance of the first groove to the stagnation point, m
$\lambda$	gas thermal conductivity, $\text{W m}^{-1} \text{K}^{-1}$
$\mu$	gas dynamic viscosity $\text{kg m}^{-1} \text{s}^{-1}$
$\rho$	gas density, $\text{kg m}^{-3}$
$\Phi$	heat transfer rate between the jet and the impinging plate, W

**Subscripts**

g	gas
j	jet
o	outlet
w	wall

**Superscripts**

'	based on $(T_j + T_o)/2 - T_w$ temperature difference
0	refers to the smooth plate

temperature  $T_j$  is measured using a thermocouple located close to the orifice (see Fig. 1).

To vary the  $R/D$  ratio, this tube ends in an orifice plate, with an orifice diameter  $D$  ranging from 2.4 to 12 mm. These orifice plate have a constant thickness  $e = 2$  mm (see Fig. 1), with a  $45^\circ$  angle chamfer, and a 1 mm chamfer thickness. However, experimental results cannot be obtained for  $R/D$  values smaller than 2, for the Reynolds number values considered in this study, because of limitations on the maximum air flow-rate delivered by the compressed air unit. The value of the  $H/D$  parameter is fixed by adjusting the orifice-to-plate distance.

The impinging surface is an aluminum circular plate with radius  $R = 24$  mm and thickness 3 mm. A high flow rate of a cooling liquid is used to maintain a fixed and uniform temperature on this impingement plate. The coolant temperature is regulated via a refrigerating unit (Huber 4 kW,  $-55/+100$  °C, stability: 0.02 °C). Under test conditions, the extracted heat rate remains lower than 2% of the cryostat capacity. Two thermocouples (Fig. 1) are inserted 1 mm under the impact surface, below the stagnation point and at the plate border. They are used to control the temperature uniformity, with a measured maximum temperature deviation of approximately  $0.5^\circ$  between the stagnation point and the plate

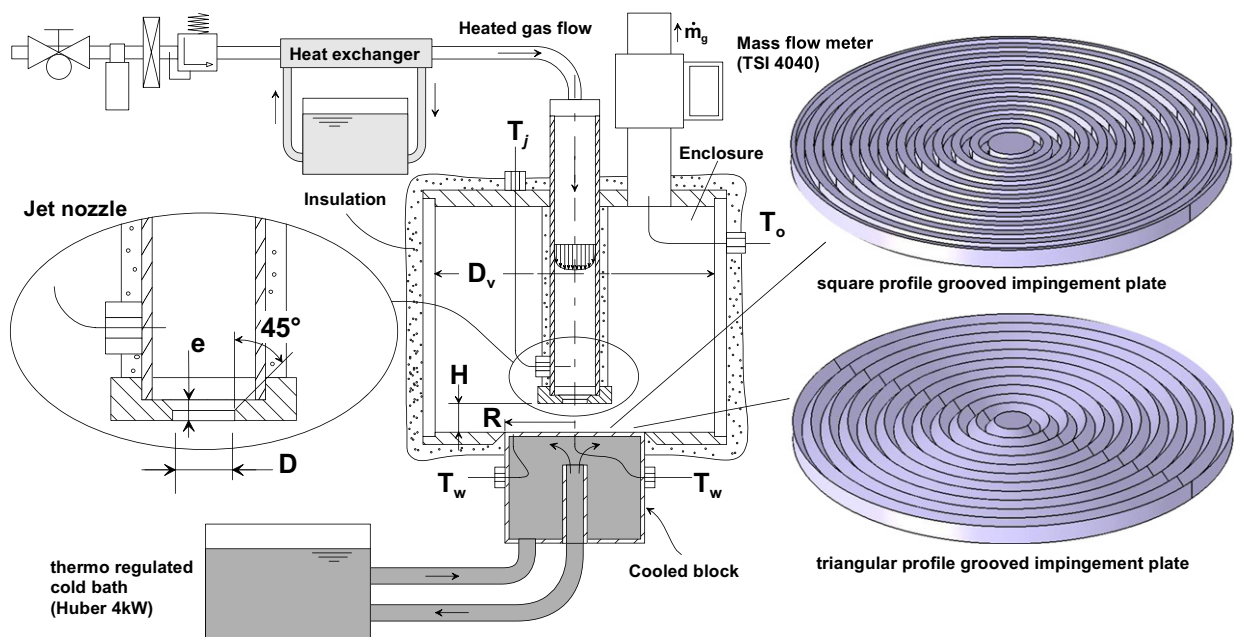


Fig. 1. Schematic of the experimental setup.

border. During the experiments the wall temperature remained close to  $T_w = 4^\circ\text{C}$ .

The hot jet enters into a PMMA cylindrical vessel with height of 200 mm, and an internal diameter  $D_v = 154$  mm. These large values of both the enclosure height and diameter permit to consider this flow configuration as axisymmetric, and minimize any possible jet confinement effects.

The enclosure gas outlet consists in a 33 mm diameter tube, located on the top of the enclosure (Fig. 1), with a thermocouple measurement of the gas outlet temperature  $T_o$ . A double hot wire anemometer (TSI 4040) is used to measure the outlet gas flow rate, together with pressure and temperature measurements, to determine the gas mass flow rate  $\dot{m}_g$ . The average jet velocity at the orifice outlet has been calculated from the mass flow-rate measurements, using appropriate values of the gas density and orifice diameter  $D$ .

In this experiment, we determine the steady heat transfer rate  $\Phi$  exchanged between the jet and the plate by using a heat balance between the inlet and outlet of the enclosure. A heat losses minimization has been carried out by having the average temperature inside the vessel close to the ambient temperature, and also by using a glass wool insulation of the enclosure. In order to keep a nearly constant temperature in the cylindrical vessel during the experiments, the gas jet temperature  $T_j$  was varied between  $40^\circ\text{C}$  and  $65^\circ\text{C}$ , depending on the flow rate. Finally, the upper part of the water cooled block, acting as the impacted plate (Fig. 1), is contactless flush-mounted with the enclosure bottom, to avoid any cold bridges. This permits to consider the enclosure as adiabatic under the test conditions.

The lathe-worked grooves have either square or triangular cross-section, with depth  $c = 1$  mm, width  $b = 1$  mm, and pitch  $p = 2$  mm (see Fig. 2). The radial distance between the stagnation point and the first groove is  $\delta/2 = 2.5$  mm. The pitch-to-depth ratio has a value  $p/c = 2$ , as chosen by Gau and Lee [7], with a groove width-to-depth ratio of  $b/c = 1$ . It should be noted (see Fig. 2) that the geometrical parameter  $b$  is the width of the lathe-worked groove for a square profile, and corresponds to the half-width of the groove for a triangular profile.

The influence of the dimensionless orifice-to-plate spacing  $H/D$  on the average heat transfer coefficient was evaluated by Sagot et al. [6], for the smooth plate configuration. Their study showed that, for  $2 < H/D < 6$ , the parameter  $H/D$  has only a weak influence on the average heat transfer. For this study with grooved impingement plates, we fixed the dimensionless orifice-to-plate ratio to  $H/D = 2$ , and the jet Reynolds numbers has been varied between 15 000 and 30 000.

The heat transfer measurements have been repeated between three and ten times, depending on the relative standard deviation of the experimental results. All the measured values of the average heat transfer coefficient were within 5% of their average value, with a mean deviation of 2%.

### 3. Data reduction

In most of the studies reported in the literature on impinging jets, the jet is at the ambient temperature  $T_o$ , since the current measurement technique is based on an imposed heat flux at the wall, together with a surface temperature distribution measurement using infra-red thermography. In this type of experiment, the reference temperature difference is chosen as  $(T_j - T_w)$ . The average jet-to-wall heat transfer coefficient is then defined as:

$$\bar{h}(R) = \frac{\Phi}{\pi R^2 (T_j - T_w)} \quad (1)$$

The average Nusselt number, based on the jet-orifice diameter  $D$ , is defined as:

$$\overline{Nu}_T = \frac{\bar{h}(R)D}{\lambda_g} \quad (2)$$

In the present study under fixed temperature conditions, the measurement of the outlet temperature  $T_o$ , for given values of  $T_j$ ,  $T_w$  and mass flow rate  $\dot{m}_g$ , permits the experimental determination of the total heat transfer rate, given by the heat balance between the inlet and outlet of the enclosure:

$$\Phi = \dot{m}_g C_p (T_j - T_o) \quad (3)$$

In this case, the reference temperature difference between the gas and the impinging plate should be defined as:  $(T_j + T_o)/2 - T_w$ . The average jet-to-wall heat transfer coefficient can then be written as:

$$\bar{h}'(R) = \frac{\Phi}{\pi R^2 \left( \frac{T_j + T_o}{2} - T_w \right)} \quad (4)$$

In our study, the corresponding average Nusselt number is defined as:

$$\overline{Nu}'_T = \frac{\bar{h}'(R)D}{\lambda_g} \quad (5)$$

with  $\lambda_g$  being evaluated at the average gas temperature.

The relationship between these two Nusselt numbers, given by Eqs. (2) and (5), can be written as:

$$\overline{Nu}_T = \overline{Nu}'_T \frac{(1+F)}{2}, \text{ with } F = \frac{T_o - T_w}{T_j - T_w} \quad (6)$$

It should be noted that for the imposed heat flux results reported in the literature,  $F = 1$ . In order to compare our results concerning the Nusselt number  $\overline{Nu}'_T$  variations with those available in the literature, it is then convenient to plot  $\overline{Nu}'_T \frac{(1+F)}{2}$ , as a function

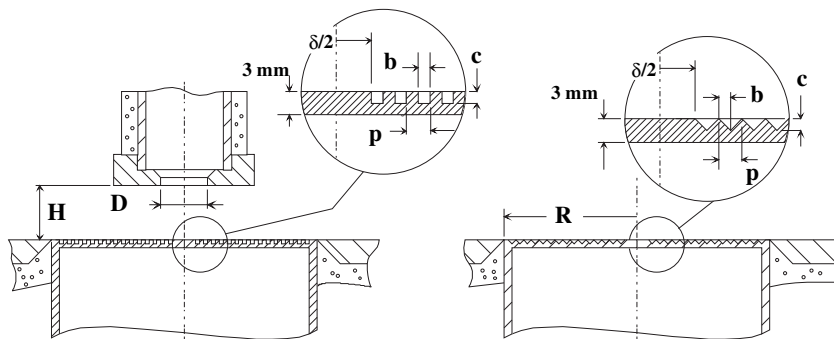


Fig. 2. Cross-sections of the impingement plates, with square and triangular grooves.

of the  $R/D$  parameter, for fixed values of the Reynolds number and of the  $H/D$  parameter.

The Nusselt number has been determined experimentally, for both a smooth plate ( $\overline{Nu}_T^0$ ) and two grooved plate configurations ( $\overline{Nu}_T$ ).

The jet average velocity  $U_j$  at the orifice plate exit was calculated as:

$$U_j = \frac{4\dot{m}_g}{\rho_g \pi D^2} \quad (7)$$

The jet Reynolds number  $Re_j$ , based on the orifice plate outlet conditions, is defined as:

$$Re_j = \frac{\rho_g U_j D}{\mu_g} = \frac{4\dot{m}_g}{\mu_g \pi D} \quad (8)$$

with  $\mu_g$  the gas dynamic viscosity, evaluated at the jet temperature  $T_j$ .

We define an intensification factor  $f = \overline{Nu}_T / \overline{Nu}_T^0$ , which is the ratio between the average Nusselt numbers obtained for grooved and smooth impinging plates, in order to evaluate the heat transfer enhancement due to the surface modification.

An uncertainty analysis on the basis of 95% confidence level of errors was carried out using the method by Kline and McClintock [10]. The analysis took into account uncertainties in the determination of the wall, inlet and outlet temperatures, the mass flow-rate measurement, the orifice plate diameter, and uncertainties on the gas thermo physical properties related to the reference temperature determination.

The maximum uncertainty in the Reynolds number  $Re_j$  was found to correspond to small values of the orifice plate diameter  $D$ , and was estimated to be 4.4% for  $R/D = 10$ , with a major contribution of the diameter value uncertainty  $\Delta D/D = 0.033$ . The minimum uncertainty of the Reynolds number was found at  $R/D = 2$  as 2.9%, with a maximum contribution of the uncertainty on the mass flow-rate measurement  $\Delta \dot{m}_g / \dot{m}_g = 0.0275$ . The maximum uncertainty in the average Nusselt number was found for  $R/D = 2$  as 4.8%. In this configuration which corresponds to a low heat transfer rate, the temperature difference ( $T_j - T_0$ ) is small, thus leading to a maximum contribution of the uncertainty on the parameter  $\Delta(T_j - T_0) / (T_j - T_0) = 0.037$ .

#### 4. Results and discussion

We present in Fig. 3 the experimental results, obtained for a jet Reynolds number  $Re_j = 23\,000$ , and for  $H/D = 2$ . A significant increase of the average Nusselt number is measured, for low values of  $R/D$ , for both the triangular and square groove profiles. For example, for  $R/D = 2$ , we obtain an increase in the average Nusselt number of 81%, as compared to the smooth plate reference configuration. This heat transfer enhancement can be attributed to secondary flows, generated inside the grooves by the radial tangential flow. The heat transfer enhancement is probably due to the local contribution to the heat removal by the vortices originating from the grooves. In case of the square grooves, the vortex is more vigorous and shedding frequently, thus causing greater heat removal from the surface, explaining why they have been shown to be more efficient than triangular grooves, as observed in Fig. 3.

One should also note that the intensification obtained with grooved plates is efficient for  $R/D$  values lower than 6–7. For increasing values of the  $R/D$  parameter, the heat transfer intensification decreases, to become negligible for values of  $R/D$  close to 10. This is obviously related to the decrease of the main flow radial velocity, when  $R/D$  increases, involving a reduction of the groove internal recirculation intensity.

In the case of smooth plate configuration, Lee et al. [3] and Baughn et al. [4] have reported local Nusselt number distributions

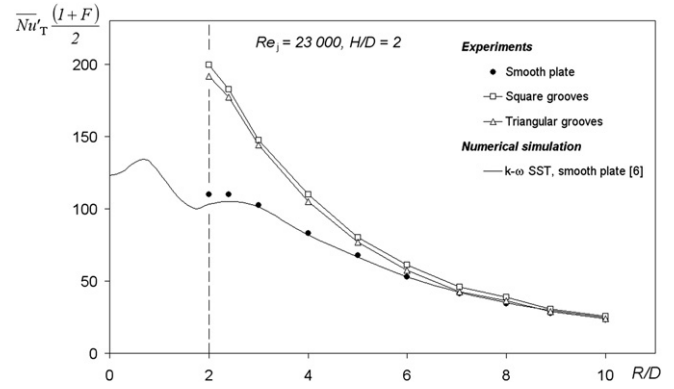


Fig. 3. Average Nusselt number obtained on smooth and grooved plates, as a function of  $R/D$ .

$Nu_T(r)$  with a secondary maximum at  $r/D$  value close to 2.2 ( $Re_j = 23\,000$  and  $H/D = 2$ ). By a spatial averaging of the local Nusselt number distribution, Sagot et al. have determined the corresponding average Nusselt number distribution, showing that the secondary maximum of the average Nusselt number distribution  $\overline{Nu}_T^0$  also occurs close to the secondary maximum of local Nusselt number distribution reported by Lee et al. and Baughn et al.

However, as mentioned in the description of the experimental apparatus, one can note that experimental results could not be obtained for  $R/D$  values lower than 2. The experimental results obtained for  $R/D > 2$  are presented along with the numerical simulation results of Sagot et al. [6]. A close agreement can be seen in Fig. 3 of present experimental results, obtained for the smooth plate reference case, with the numerical simulation results of Sagot et al. For  $R/D$  close to 2, the experimental measurements for the smooth plate configuration are consistent with the existence of a secondary maximum, observed in the numerical study.

We report in Fig. 4 the variations of the intensification factor  $f = \overline{Nu}_T / \overline{Nu}_T^0$ , for both square and triangular grooves. Within the experimental uncertainties, this intensification factor  $f$  appears to be independent to the Reynolds number, in the considered range  $15\,000 \leq Re_j \leq 30\,000$ . However, the grooves with a square profile appear to be more efficient than those with a triangular profile, for the jet-to-wall heat transfer enhancement, under constant temperature wall conditions.

It may be noted that the intensification factor  $f$  obtained experimentally tends towards 1, for high  $R/D$  values. This demonstrates the weak effect of the grooves on the heat transfer for increasing  $R/D$  values.

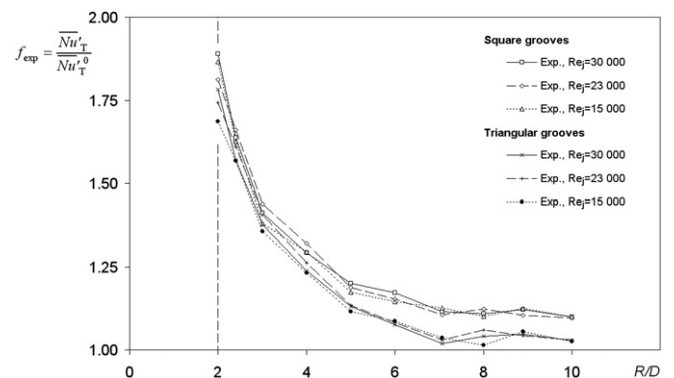


Fig. 4. Heat transfer enhancement for various grooves and jet Reynolds number values.

The intensification factor  $f$ , obtained with the utilization of axisymmetric grooves on the impinging plate, can be expressed as:

$$f = 1 + K \left( \frac{R}{D} \right)^n \quad (9)$$

The coefficients  $n$  and  $K$  have been obtained by a least squares minimization. Their values are  $-1.52$  and  $2.4$ , respectively, for the square grooves, and  $-1.95$  and  $3$ , respectively, for the triangular profile grooves. Eq. (9) is valid for  $15\,000 \leq Re_j \leq 30\,000$ ,  $H/D = 2$ , and  $2 \leq R/D \leq 10$ . The mean relative deviation of the experimental values from those given by Eq. (9) is 2%, with a maximum deviation of 5%.

An average Nusselt number correlation for a smooth plate  $\overline{Nu}_T^0(Re_j, R/D, H/D)$  has been previously proposed by Sagot et al. [6]. By combining this correlation, for  $H/D = 2$ , with the relation between  $\overline{Nu}_T$  and  $\overline{Nu}'_T$  given by Eq. (6), together with Eq. (9) for the intensification factor, we obtain an expression of the average Nusselt number for grooved plate configurations, in the following form:

$$\overline{Nu}'_T = 0.0588 Re_j^{0.8} \left[ 1 - 0.168 \left( \frac{R}{D} \right) + 0.008 \left( \frac{R}{D} \right)^2 \right] \left( \frac{\mu_j}{\mu_w} \right)^{0.25} \times \frac{2}{1+F} \left[ 1 + K \left( \frac{R}{D} \right)^n \right] \quad (10)$$

The viscosity ratio  $\mu_j/\mu_w$  is based on the jet and wall temperatures, with  $F$  defined in Eq. (6). Values of  $K$  and  $n$  depend on the type of the groove. The correlation can be utilized for the determination of the average heat transfer coefficient  $\overline{h}(R)$ , for  $H/D = 2$ ,  $15\,000 \leq Re_j \leq 30\,000$ , and  $2 \leq R/D \leq 10$ . As this correlation is based on an average temperature difference  $(T_j + T_0)/2 - T_w$ , an iterative procedure that combines Eqs. (3)–(5) and (10) must be used.

## 5. Conclusion

Gas-to-wall heat transfer enhancement in an impinging jet flow with axisymmetric grooves on the plate surface under constant wall temperature conditions has been studied. Square grooves have been found to be more efficient, for heat transfer intensification, than those with a triangular profile. The intensification is found to be effective only for  $R/D$  values lower than approximately 6.

Correlations of the intensification factor for impingement grooved surfaces (the ratio of the average Nusselt number values for grooved and smooth plates) and average Nusselt number have been developed, which are valid in the range  $15\,000 \leq Re_j \leq 30\,000$ , for  $2 \leq R/D \leq 10$  and  $H/D = 2$ , for the two groove types studied.

## References

- [1] D. Lytle, B.W. Webb, Air jet impingement heat transfer at low nozzle-plate spacings. *Int. J. Heat Mass Transf.* 37 (12) (1994) 1687–1697.
- [2] M. Fenot, J.-J. Vullierme, E. Dorignac, Local heat transfer due to several configurations of circular air jets impinging on a flat plate with and without semi-confinement. *Int. J. Thermal Sci.* 44 (2005) 665–675.
- [3] D.H. Lee, S.Y. Won, Y.T. Kim, Y.S. Chung, Turbulent heat transfer from a flat surface to a swirling round impinging jet. *Int. J. Heat Mass Transf.* 45 (2002) 223–227.
- [4] J.W. Baughn, A.E. Hechanova, X. Yan, An experimental study of entrainment effect on the heat transfer from a flat surface to a heated circular impinging jet. *J. Heat Transf.* 113 (1991) 1023–1025.
- [5] F.P. Incropera, D.P. De Witt, T.L. Bergman, A.S. Lavine, *Fundamentals of Heat and Mass Transfer*, sixth ed. Wiley, New York, 2007, pp. 447–452.
- [6] B. Sagot, G. Antonini, A. Christgen, F. Buron, Jet impingement heat transfer on a flat plate at a constant wall temperature. *Int. J. Thermal Sci.* 47 (12) (2008) 1610–1619.
- [7] C. Gau, I.C. Lee, Flow and impingement cooling heat transfer along triangular rib-roughened walls. *Int. J. Heat Mass Transf.* 43 (2000) 4405–4418.
- [8] S.S. Hsieh, H.H. Tsai, S.C. Chan, Local heat transfer in rotating square-rib-roughened and smooth channels with jet impingement. *Int. J. Heat Mass Transf.* 47 (2004) 2769–2784.
- [9] N. Gao, H. Sun, D. Ewing, Heat transfer to impinging round jet with triangular tabs. *Int. J. Heat Mass Transf.* 46 (2003) 2557–2569.
- [10] S.J. Kline, F.A. McClintock, Describing uncertainties in single sample experiments. *Mech. Eng.* 75 (1953) 3–8.